JOURNAL OF THERMOPHYSICS AND HEAT TRANSFER
Vol. 11, No. 3, July–September 1997

Evaluation of Real-Gas Phenomena in High-Enthalpy Aerothermal Test Facilities: A Review

Chul Park*
Tohoku University, Sendai 980-77, Japan

The methods of making more accurate measurements in arcjet wind tunnels in the real-gas regime than have been achieved up to the present time are explored by reviewing, comparing, and interpreting the existing experimental methodologies and obtained data. The inaccuracies of the conventional method of determining enthalpy and flow uniformity are first pointed out. The extent and consequences of flow contamination by copper vapor are next examined. Then the data obtained through spectroscopic determination of flow enthalpies, Doppler velocimetry using laser-induced fluorescence, and species concentration determination using mass spectrometry are reviewed. The discrepancies between the measured and calculated flow velocities and species concentrations are pointed out and a possible explanation is given.

Nomenclature

A = nozzle cross-sectional area, m^2
C_p = specific heat at constant pressure
C_v = specific heat at constant volume
D = diameter of constrictor, m
d = diameter of model, m
H = enthalpy, J/kg
h_i = chemical energy of species i, J/mol
L = length of constrictor, m
n_i = species concentration, mol/kg
p = pressure, Pa
$\dot{q}$ = stagnation-point heat transfer rate, W/m^2
r = radial distance, m
T = heavy particle temperature, K
T_e = electron temperature, K
T_v = vibrational temperature, K
U = freestream velocity, m/s
u = velocity in radial direction, m/s
v = vibrational quantum number
y = distance normal to wall, m
γ = specific heat ratio C_p/C_v
ρ = density, kg/m^3
σ = vibrational energy, J/kg

Subscripts
av = average
c = centerline
e = boundary-layer edge
s = pitot total
0 = reservoir
∞ = freestream
* = nozzle throat

Introduction

SINCE the dawn of the space age in the 1950s, there has been a need for temperature-resistant materials to be used for the heat shields for the re-entry vehicles and launch systems. These heat shield materials had to be tested in the high heating environments encountered in flight. The flows around such vehicles reach a temperature of up to 7000 K. For the vehicles entering other planets, the temperature reaches 14,000 K. At such temperatures, air becomes vibrationally excited, dissociated, and ionized. These chemical reactions absorb heat, and thereby significantly affect the heat transfer rates. For this reason, it was deemed necessary that the facility to test such materials reproduce the temperatures of the gas flows as well as the heat transfer rates.

There are no other means of producing such a high-temperature gas under a steady-state condition than electrical-discharge heating. For this reason, various types of electrical discharge-heated wind tunnels, commonly called arcjet wind tunnels, have been constructed since the late 1950s. Since the mid-1970s, only one specific design, the segmented constrictor, has emerged in the U.S. as the most widely used wind-tunnel design for producing the flow environments of the orbital re-entry conditions.[1]

These arcjet wind tunnels have been used in developing the heat shield materials for the Space Shuttle Orbiter and planetary entry vehicles such as Pioneer–Venus Probes and the Galileo Probe. In the utilization of those wind tunnels, there always was a question about the accuracy of the data obtained. Uncertainty existed on 1) enthalpy level, 2) freestream conditions, and 3) accuracy of the theoretical procedures to determine flow variables at the surface of the tested models. Because of these uncertainties, heat shields are designed with a certain safety margin.

The safety margin represents unnecessary weights and reduction in payload performance of the vehicle. Therefore, efforts have been expended over the years to eliminate those uncertainties through accurate characterization of the flows produced in the facilities. The state of the art prior to 1992 was reviewed in Ref. 2.

In the present work, a similar review is made intending to augment Ref. 2 by incorporating the data obtained since 1992. The methodologies and the results pertaining to the three previously mentioned issues are described and evaluated. In the areas where the experimental data differ from the theoretical predictions, a possible explanation is given.

Basics of Arcjet Wind Tunnel

Construction and Operation

A segmented constrictor-type arcjet wind tunnel consists of four main parts: 1) an upstream electrode chamber, 2) a con-

Received May 17, 1996; presented as Paper 96-2207 at the AIAA 27th Fluid Dynamics Conference, New Orleans, LA, June 17–20, 1996; revision received Jan. 23, 1997; accepted for publication Jan. 24, 1997.

*Professor, Department of Aeronautics and Space Engineering. Associate Fellow AIAA.

strictor tube, 3) a downstream electrode chamber, and 4) a convergent–divergent nozzle. A set of electrodes is housed in the two electrode chambers. The downstream electrode chamber functions as the reservoir for the wind tunnel. The test gas is introduced both from the upstream electrode chamber and the constrictor wall, and is made to flow out through the nozzle. Since the constrictor diameter is larger than the diameter of the nozzle throat, the flow through the constrictor is subsonic. A dc electric discharge is made between the electrodes through the test gas flowing inside the constrictor. The test gas is heated by this electric discharge.

The electrodes are made of copper and formed into the shape of a ring. A magnetic field is applied to each electrode ring to rotate the position of arc attachment. One electrode ring can carry a maximum current of about 500 A. The number of electrode rings is determined by the desired electrical current. Since the anodes are heated more than the cathodes from the bombardment of electrons, they are placed in the upstream where the test gas is cold. The conductivity of the heated test gas is such that a voltage gradient of 20–40 V/cm is formed. To prevent the electrical current from shorting through the constrictor wall, the constrictor tube is made by a lamination of copper disks of about 1 cm thickness. Each constrictor disk is electrically insulated from the neighboring disk by a thin nonconducting disk. All components are water cooled.

From the upstream electrode chamber, usually a small amount of argon is introduced to provide the necessary electrical conductivity at an unheated condition. Most of the test gas mass is introduced from small holes drilled through the insulator disks. D is chosen such that the heat transfer rate to its wall is kept below an acceptable level, usually about 50 MW/m^2. L is chosen to satisfy the following two criteria:

1) The heating process reaches steady state at the end of constrictor; i.e., a balance is reached between the electrical power input and the heat transfer rate to the wall. This means that the enthalpy of the gas flow will not increase even if the constrictor is made longer.

2) The electric discharge is stable in that the voltage gradient remains constant, so that no instantaneous high-voltage gradient occurs to cause high local heating and electrical shorting between neighboring pairs of constrictor disks.

The first criterion is probably satisfied with an L/D of about 25 (Ref. 3). However, the second criterion requires L/D to be larger. As a result, the L/D is chosen to be between 35–50. For a large arcjet wind tunnel, an L/D of 50 results in a total required voltage of about 20 kV. The largest arcjet wind tunnel in existence operates at 20 kV and 3 kA, resulting in a power consumption of 60 MW (Ref. 1).

When the pressure in the constrictor is low, i.e., of the order of 1 atm, the electric discharge occurs diffusely; i.e., the electrical current path occupies almost the entire volume within the constrictor and is steady. As the pressure is raised, the diameter of the current path becomes smaller and unsteady. At a pressure of about 100 atm, the diameter of the current path is only about 10% of the constrictor diameter.[4] At a higher pressure, the current extinguishes. The maximum operating pressure is set by this phenomenon to be about 200 atm.

Since the mass flow rate of the test gas is proportional to the pressure inside the constrictor, a high pressure implies a high mass flow rate. Because the total electrical power input is determined by the wall-cooling capacity and therefore is relatively independent of the operating pressure, a high pressure implies a low enthalpy of the test gas flow. To produce a test gas flow in the dissociated or ionized regime, an arcjet wind tunnel must be operated at a constrictor pressure below about 10 atm.

The electrical power level presently attained, 60 MW, is much lower than the power level a shock tunnel delivers during its short run time. To provide the Reynolds numbers occurring in flight at a hypersonic Mach number, a hypersonic facility must operate at very high reservoir pressures in addition to high enthalpies. A large shock tunnel is capable of operating at a reservoir pressure of about 1000 atm at an enthalpy of up to about 20 MJ/kg for a short time. The energy flow rate, $\rho_* U_* H A_*$, for such a facility is more than 1 GW during the flow duration. With an available power of 60 MW, it is unrealistic to expect an arcjet wind tunnel to provide such hypersonic flow conditions.

Because the diameter of the nozzle throat is usually significantly smaller than the diameter of the constrictor (the facility at NASA Johnson Space Center is an exception), the flow inside the reservoir moves with a low subsonic speed. Hence, it is very likely that thermochemical equilibrium is reached at the entrance to the nozzle.

Average Enthalpy

By measuring the total rate of the water flow through the cooling passages of all components and the average temperature rise in the water, one can determine the magnitude of the heat removed through wall cooling. By subtracting this cooling loss from the input electrical power, one determines the net power input into the gas. By dividing the net power input by the flow rate of the test gas, one obtains an average of the enthalpy of the test gas H_{av}, which is sometimes called the energy balance enthalpy. The ratio of the net power output to the total power input is called the heater efficiency. The efficiency is usually about 40% or larger.

Even though the electrical current path fluctuates, on the average it passes through the central axis of the constrictor. As a result, the enthalpy distribution of the test gas at the exit of the constrictor is highly peaked at the center; i.e., the ratio H_c/H_{av} is significantly larger than 1. A computer code has been developed to calculate the flow properties in the constrictor using several approximations.[5] According to the calculations made using the code, the enthalpy value at the centerline is indeed much higher than the average value. A spectroscopic measurement of the flow in the constrictor near its exit[6] shows that, at the constrictor pressures below 6 atm, the flow properties are approximately as the code predicts.

In the reservoir, which functions as the downstream electrode chamber, a mixing phenomenon occurs, and so the enthalpy distribution is modified. It is possible that enthalpy distribution is less peaked at the nozzle entrance than at the constrictor exit. Efforts have been made in the past to calculate the flow processes in the reservoir.[7,8] However, no reliable method has yet been developed to determine the flow property distribution in the radial direction at the nozzle entrance.

Because the radial distribution of flow properties is unknown at the nozzle entrance, there are no ways of predicting the radial flow property distribution at the nozzle exit. Because the gas density is high in the cold boundary layer over the nozzle, one suspects that a significant fraction of the total mass flow rate is in the cold region. This is another reason why one suspects that enthalpy is peaked at the center.

Basic Diagnostics

Most basic diagnostics of an arcjet wind-tunnel flow consist of radial surveys of pitot total pressure, $p_s \approx \rho_\infty U_\infty^2$, and heat transfer rate to the stagnation point of a sphere, $\dot{q} \approx$ a constant $\times \sqrt{\rho_\infty U_\infty H}$. Usually, both p_s and $\dot{q}$ are found to be nearly constant in the radial direction over more than half the nozzle radius. This is not a proof that the flow properties are uniform over that range of radius, for the following reasons:

Enthalpy distribution in the radial direction can be written in the central inviscid core region generally by a parabola

$$H/H_c = 1 - C_1 r^2$$

In the inviscid region of the nozzle flow, expansion occurs along each streamline satisfying the momentum equation

$$d\left(\frac{U^2}{2}\right) = -\frac{dp}{\rho}$$

The result of integration of this equation can be written as

$$U_\infty^2/2 = (p_0 - p_\infty)/\rho_{av}$$

From this, one can write

$$p_s \approx \rho_\infty U_\infty^2 = 2(p_0 - p_\infty)(\rho_\infty/\rho_{av})$$

The density ratio ρ_∞/ρ_{av} is a function of the effective area ratio, and, therefore,

$$p_s = (p_0 - p_\infty) \times \text{a function of area ratio}$$

Since $p_0 - p_\infty$ is approximately constant across the inviscid core, p_s is nearly constant regardless of how the enthalpy distribution is peaked, i.e., regardless of the magnitude of the curvature C_1.

Because enthalpy is distributed parabolically, the exit velocity U is expected also to be parabolically distributed. In a real-gas regime, U is not necessarily proportional to $\sqrt{H}$, and so one should write its radial distribution in the inviscid core in a general form

$$U/U_c = 1 - C_2 r^2$$

The radial distributiion of mass flow rate $\rho_\infty U_\infty$ then becomes

$$\frac{\rho_\infty U_\infty}{\rho_{\infty_c} U_{\infty_c}} = \frac{\rho_\infty U_\infty^2}{\rho_{\infty_c} U_{\infty_c}^2} \frac{U_{\infty_c}}{U_\infty} = \frac{1}{1 - C_2 r^2}$$

for the region $C_2 r^2 < 1$. There follows

$$\frac{\dot{q}}{\dot{q}_c} \approx \frac{\sqrt{\rho_\infty U_\infty} H}{\sqrt{\rho_{\infty_c} U_{\infty_c}} H_c} = \frac{1 - C_1 r^2}{\sqrt{1 - C_2 r^2}} \approx 1 - (C_1 - C_2/2) r^2 + 0(r^4)$$

Thus, the radial variation of $\dot{q}$ is milder than that of either H or U. If by coincidence $C_2/2$ is equal to C_1, the $\dot{q}$ distribution will be flat. Thus, both p_s and $\dot{q}$ can be either flat or nearly flat even when H and U are peaked at the center.

The mass flow rate and enthalpy could be measured in principle using a so-called flow-swallowing device.[9] In this device, a sharp-lipped tubing is made to swallow the oncoming flow. The mass flow rate through the tube is metered using a Venturi-tube arrangement. The flow enthalpy is determined by measuring the temperature rise in the cooling water and dividing the cooling loss by the gas mass flow rate. In practice, metering the flow rate through the device is very difficult because of viscosity. Enthalpy determination is equally difficult because most of the heat transfer to the wall occurs around the lip, and because one cannot determine what fraction of the heat collected in the cooling water is from the outer wall of the lip.

Attempts have been made in the past to determine enthalpies from the measured values of mass flow rate and reservoir pressure.[10] In an inviscid flow, the mass flow rate through the sonic throat is a unique function of enthalpy and reservoir pressure. Therefore, enthalpy can be deduced from the measured mass flow rate and the pressure. The enthalpy value so obtained is usually approximately equal to the enthalpy value determined through heat transfer rate measurement.[2] However, the basic assumption of inviscid flow is not satisfied in an arcjet flow, and hence, the method cannot be considered accurate.

Copper Vapor

The electrodes and the constrictor disks are both made of copper. During the operation of an arcjet tunnel, these parts can vaporize and inject copper vapor into the test stream. The electrodes erode at such a rate that every few months they need to be exchanged with new ones. By weighing the electrodes before and after their use, one can determine the average rate of their erosion. From this, one can deduce the average concentration of copper vapor in the test stream. The erosion rate of the electrodes has also been calculated theoretically.[7,8] The calculated values agree roughly with the measured values.

If the electrical discharge through the constrictor is steady and if the resulting wall heat transfer rate is below about 50 MW/m^2, the constrictor walls do not erode at all. Erosion occurs only when the local heat transfer rate attains instantaneously a very high value because of the fluctuation of the electrical discharge. In a device with a large L/D, i.e., larger than about 40, such fluctuations do not occur, and hence, the wall erosion is negligible. When operated at a pressure of about 100 atm in the constrictor, an arcjet tunnel produces copper vapor to a concentration of about 200 ppm by mass, or about 100 ppm by mole.[4] At a lower pressure, the copper concentration is less.

The extent of copper contamination can be determined also by observing the radiation emitted from the shock layer over a blunt body. In Fig. 1, one such example spectrum is shown.[11] The spectrum was obtained at an enthalpy of about 28 MJ/kg and at a reservoir pressure of 1.4 atm. The copper lines at 324.7 and 327.4 nm were the only copper lines seen in that experiment over the observed wavelength range from 240 to 900 nm. By comparing the intensities of these copper lines with those of air species, copper content is determined to be

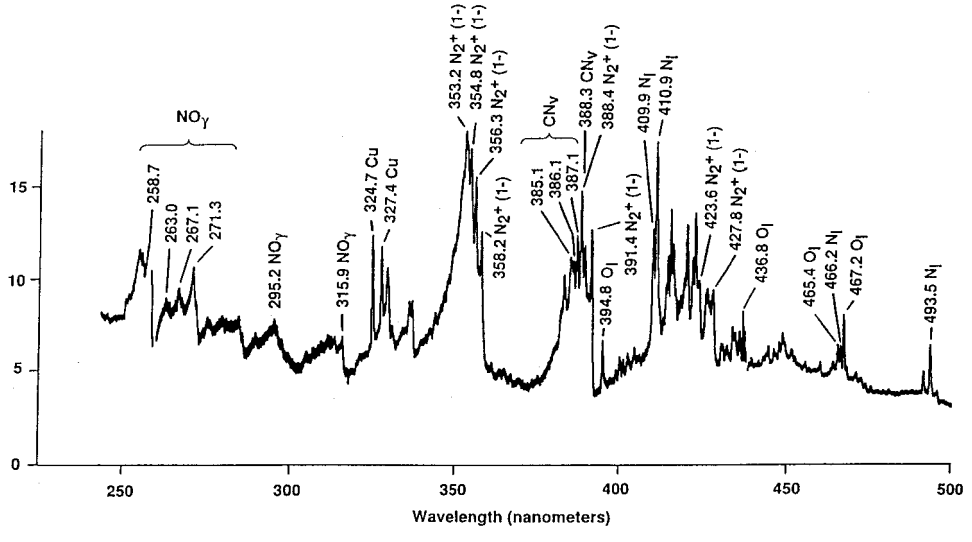

Fig. 1 Shock-layer radiation incident on the stagnation point obtained in an arcjet wind tunnel.[11]

of the order of 0.1 ppm for this case. The copper lines were so weak that the attempt to use the lines for velocity measurement via the laser-induced fluorescence was not successful.[12]

The very low concentration of copper vapor in the example shown is achieved, for the reasons given earlier, only when L/D is sufficiently large, the nozzle throat diameter is sufficiently smaller than the constrictor diameter, and the operating pressure is low. In an experiment with a tunnel having an L/D of about 35 and a nozzle throat diameter larger than the constrictor diameter, the copper lines appeared much stronger.[13,14]

Copper vapor could affect the thermochemistry of the test gas. However, at a concentration below 100 ppm, its extent is likely to be negligibly small. In the reservoir, the equilibrium condition dictates that the copper vapor exists either in its neutral atomic state, Cu, or ionized state, Cu^+. During the expansion, Cu^+ will tend to ionically recombine into Cu, but some Cu^+ will remain unrecombined at the nozzle exit. The presence of Cu^+ in the test section will contribute to keeping the electron density high there, and thereby promotes equilibrium among various electronic states of the gas species present.

The only stable molecule neutral copper atom that could form in an arcjet wind tunnel is CuO. However, its binding energy is relatively low, i.e., only 2.87 eV. As a result, if it is formed, it tends to be reduced back to Cu by collisions with O and N atoms through the exothermic exchange processes

$$CuO + O \rightarrow Cu + O_2 + 2.21 \text{ eV}$$

$$CuO + N \rightarrow Cu + NO + 4.18 \text{ eV}$$

Thus, Cu will exist mostly in its atomic form, and will not participate meaningfully in any chemical reactions involving air species.

The copper vapor could condense on the model wall, and thereby change its catalycity. However, in most cases, the wall is heated to a temperature of about 1000 K or higher. At such a temperature, condensed copper vapor evaporates from the surface. As a result, during the operation of the facility the copper vapor is not likely to affect the surface catalycity. Only during the process of shutting down a tunnel can one recognize condensation of copper on the surface because of the accompanying color change.

Enthalpy Determination

Heat Transfer Measurement

It is a common practice to determine the enthalpy of the flow from $\dot{q}$ through the use of the formulas of Fay and Riddell[15] and of Goulard.[16] The formula of Fay and Riddell[15] gives the heat transfer rate to a fully catalytic wall. The formula of Goulard[16] provides the correction necessary to account for the finite surface catalycity.

The two formulas are based on the following assumptions:

1) The radial acceleration of the inviscid shock layer at the boundary-layer edge, du_e/dr, is that of the Newtonian flow.

2) The vorticity of the boundary-layer flow, du/dy, is zero at the boundary-layer edge.

3) The flow is in equilibrium at the boundary-layer edge.

4) The flow is frozen in the boundary layer.

Of these, assumptions 1, 2, and 4 are usually violated in an arcjet wind tunnel. Assumption 3 may or may not be satisfied, depending on p_s and d.

The shock-layer thickness in an arcjet wind tunnel always appears much thicker than that observed in flight. This is because 1) the flow Mach number is usually too low for the flow to be hypersonic, and 2) the presence of dissociated species in the test stream causes the effective γ to be large. As a result, the Newtonian approximation is inaccurate for most arcjet conditions.

The Reynolds numbers attainable in an arcjet wind tunnel in the real-gas regime are usually too small for assumption 2 to be satisfied. The radial velocity in the shock layer varies across the shock layer. The velocity immediately behind the bow shock is about twice that at the boundary-layer edge. As a result, there is a finite vorticity in the inviscid region of the shock layer. The vorticity of the boundary-layer flow must equal this vorticity value at the boundary-layer edge.

The time required for shock-heated air to reach equilibrium is known from the experiments conducted in a shock tube.[17] According to the data, equilibrium is not likely to occur in most of the high-enthalpy tests conducted in an arcjet wind tunnel. However, the presence of dissociated and excited species in the freestream reduces the required time significantly. As a result, assumption 3 may be satisfied provided the p_s and d satisfy a certain condition. This point will be elaborated on later.

The density of the boundary-layer flow is usually too low for three-body recombination processes to proceed, as pointed out by Goulard.[16] However, the density is usually sufficiently high for the Zeldovich reactions $O + N_2 \rightleftharpoons NO + N$ and $O + NO \rightleftharpoons O_2 + N$ to proceed. Because of these reactions, the wall values of O and N atoms and NO molecules are different from those assumed in the theory of Goulard.[16]

For these reasons, flow enthalpy values cannot be deduced accurately from the measured $\dot{q}$ values through the use of the Fay and Riddell[15] and Goulard[16] formulas. In many cases, the centerline enthalpy value deduced from $\dot{q}$ agrees approximately with the average enthalpy value. Such agreement should not be considered to be the proof of validity of either methods, because, as mentioned earlier, the centerline enthalpy is different from the average enthalpy. Therefore, it becomes necessary to determine the flow enthalpy through an independent measurement. In principle, one could observe the radiation spectrum emanating from the nozzle entrance region of an arcjet and analyze it to determine enthalpy distribution. Such a measurement has not yet been made.

Spectroscopic Method

One successful method of measuring enthalpy is through the use of optical spectroscopy. In this method, the radiation emanating from the shock layer over a blunt body placed in the test section is observed from the side-on position, i.e., from the direction normal to the nozzle axis. If the shock layer is in equilibrium, then enthalpy can be determined by analyzing the spectrum obtained. The ratio of the flow residence time in a shock layer to the time required for chemical reactions to complete is proportional to the product $p_s d$, and so equilibrium will exist when the product is sufficiently large. Since the gas property varies radially as well as axially in the shock layer, an Abel inversion (see, e.g., Ref. 18) would be necessary in principle. However, in practice, a fairly accurate enthalpy value can be obtained even without Abel inversion if the blunt body is a flat circular disk. This is because 1) enthalpy is nearly constant over half the radius in the shock layer over a flat disk, and 2) radiation intensity is a very strong function of enthalpy, and therefore, the observed radiation is strongly weighted toward the central region.

This technique was used in Refs. 19–23. In all of these measurements, observation was made with a flat disk from the side-on direction. The operating parameters are compared in Table 1. As seen in Table 1, the product $p_s d$ was approximately the same among the first three experiments. The $p_s d$ value for

Table 1 Operational parameters in spectroscopic determination of enthalpy through observation of a flat disk shock layer

Reference	Year	Gas	d, cm	p_s, atm	$p_s d$, atm-cm	Equilibrium/ nonequilibrium
19	1970	N_2	2.5	0.3	0.75	Equilibrium
20	1973	N_2	5	0.1	0.5	Equilibrium
22	1995	Air	15	0.028	0.42	Equilibrium
23	1989	N_2	10	0.016	0.16	Nonequilibrium

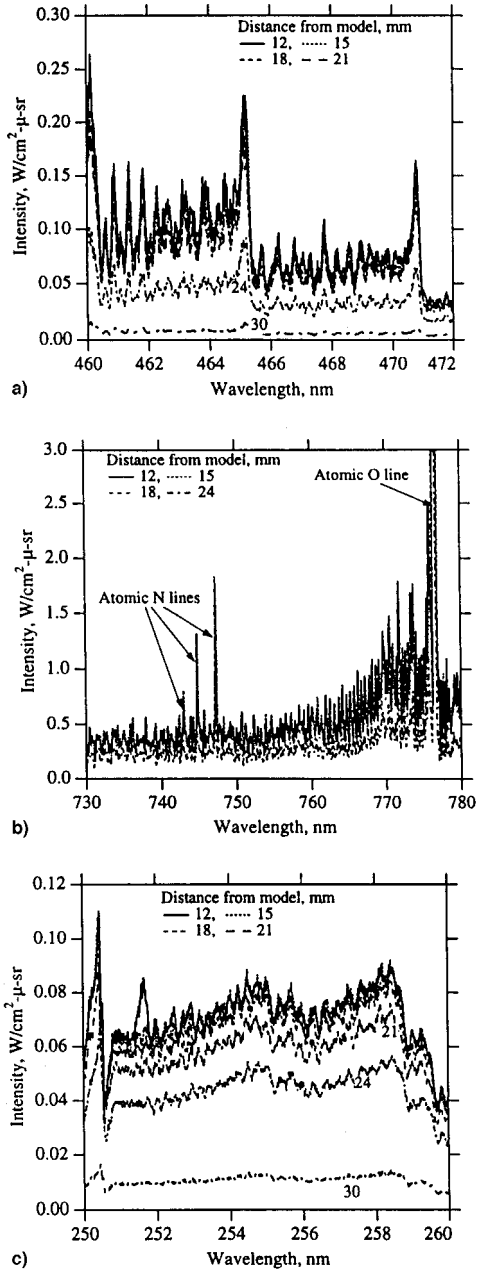

Fig. 2 Spectra from a shock layer over a flat disk,[22] $p_s d$ = 0.42 atm-cm: a) N_2^+ first negative band system, b) atomic N and O lines and background radiation, and c) NO band system.

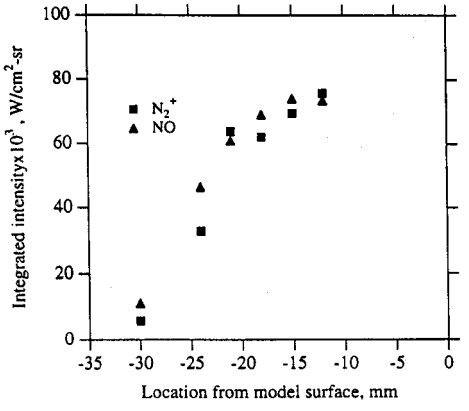

Fig. 3 Integrated intensities of N_2^+ and NO radiations,[22] $p_s d$ = 0.42 atm-cm.

the fourth experiment[23] was about one-third or less of those in the first three. In Refs. 20, 22, and 23, the radiation measurement was made at several different lines of sight located at different distances away from the wall. The results for the third experiment are reproduced in Fig. 2.

As seen here, the spectra are qualitatively identical at 12, 15, and 18 mm away from the model surface; they differ only in intensity. In Fig. 3, the intensities of N_2^+ and NO band systems are compared. Their intensities vary, but the ratio of intensities between the two band systems remain approximately constant. This proves that the thermodynamic state variables are the same among those three locations. The ratio of intensity of atomic lines of nitrogen or oxygen to that of N_2^+ or NO band behave similarly.[22]

The fact that an equilibrium region exists for the condition shown deserves attention. The observed equilibration distance is only 1/20 of the equilibration distance in an undisturbed air.[17] This can be attributed to the existence of dissociated and electronically excited species.

In Fig. 4, the intensity ratios between the atomic nitrogen lines at 742–747 nm and the N_2^+ first negative bands are shown as a function of enthalpy. As seen here, the intensity ratio is a strong function of enthalpy. A 10% error in the determination of intensity ratio results in only 2.5% error in enthalpy. A similar relationship exists between atomic nitrogen lines and NO bands. In the cases where enthalpy is too low for the nitrogen lines to emit significant radiation, the atomic oxygen line at 777 nm can be used instead, with a similar degree of accuracy.

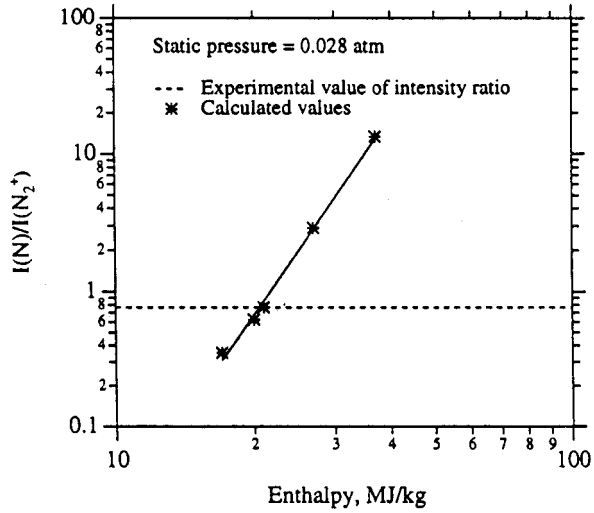

Fig. 4 Relationship between spectral intensity ratio and enthalpy under equilibrium.[22]

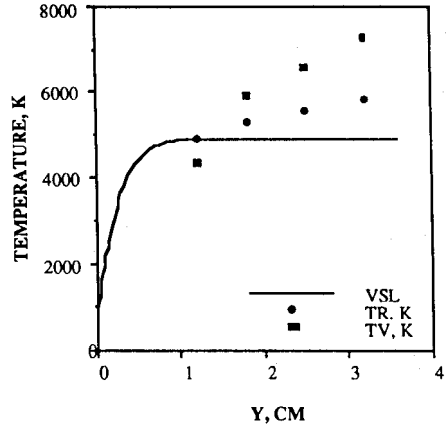

Fig. 5 Measured rotational and vibrational temperatures,[23] $p_s d$ = 0.16 atm-cm.

The rotational and vibrational temperatures in the shock layer determined in the fourth experiment[23] are reproduced in Fig. 5. As seen here, the temperatures did not reach a steady state within the shock layer, signifying that equilibrium was not reached. The difference between this case and the case shown in Figs. 2–4 is the magnitude of the $p_s d$ product. It was too small for equilibrium to be reached in this experiment.

Freestream Flow Properties

In the cases where the density of the test gas and the size of the facility is such that the product $p_s d$ is below about 0.4 atm-cm, spectroscopic enthalpy determination is not possible, as seen earlier. In such a case, the flow enthalpy must be determined through the measurement of each component in the enthalpy expression

$$H = C_p T + U^2/2 + \sigma(T_v) + \sum n_i h_i$$

The magnitude of each component in this expression must be determined also if the experimental environment is such that the flow does not reach equilibrium at the edge of boundary layer over the tested model. This is because, in such a case, the flow variables at the model surface must be calculated employing an elaborate computational fluid dynamic technique, and, to do so, the freestream conditions must be known in detail.

Velocity Measurement

The velocity of the flow in the test section of an arcjet wind tunnel has been measured, among others, by Marinelli et al.[14] and Bamford et al.[12,24] In both measurements, the Doppler effect for a laser-induced fluorescence line was the principle of measurement. Marinelli et al.[14] applied the technique to a copper line because it was the most prominent radiation feature; Bamford et al.[12,24] used an atomic oxygen line because a copper line was too weak to be reliable. The two results are compared in Figs. 6a and 6b.

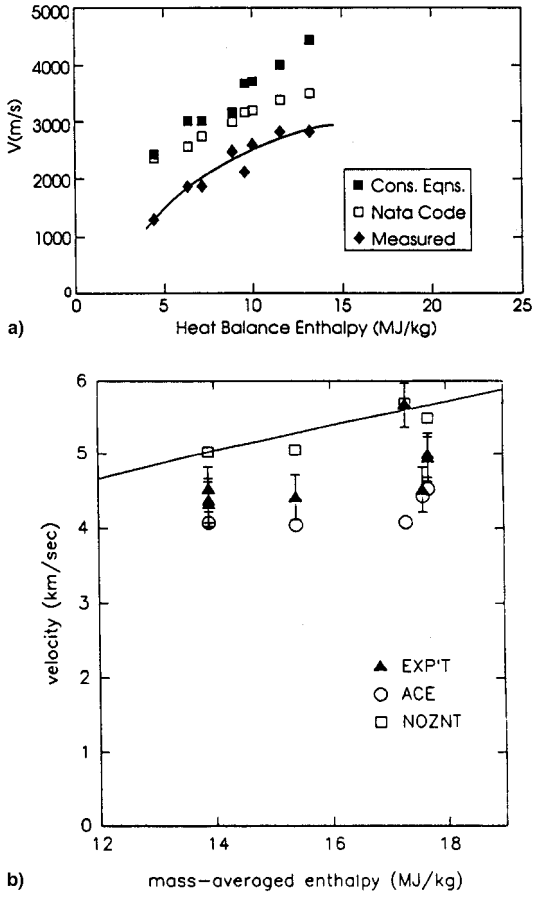

Fig. 6 Comparison between the measured and calculated velocities: a) Marinelli et al.[14] and b) Bamford et al.[12]

In both of these figures, the abscissa is the average enthalpy. The measured data are compared with the calculations made with several different methods. Although these calculation methods are different, they predict approximately the same values at the overlapping enthalpy of 14 MJ/kg. At that enthalpy, the velocity measured by Bamford et al.[12,24] is nearly 1.4 times that obtained by Marinelli et al.[14] The velocity values measured by Bamford et al.[12,24] are slightly smaller than the calculated values. The values obtained by Marinelli et al.[14] are considerably smaller than the calculated values. This discrepancy could be attributed partly to the difference in the facilities and partly to the difference in the gas species for which the laser-induced fluorescence technique was applied.

Internal Temperatures

The vibrational temperature of N_2 has been measured in air in an arcjet wind tunnel by MacDermott and Marshall[25] using an electron-beam excitation technique. The measured vibrational temperature values are compared with the calculated values in Fig. 7. In the figure, the solid curve represents the calculation made using a five-temperature model,[26] while the dash curve is a calculation by MacDermott and Marshall[25] using a four-temperature model in which vibrational temperatures of the three molecular species are accounted for but the electron–electronic temperature was not separately calculated. As seen here, the five-temperature description brings a closer agreement with the experimental data.

The vibrational temperature of NO was measured in Ref. 27 using an absorption technique. A beam of continuum radiation was passed across the nozzle, passing through the cold boundary layers. The absorption by the $v = 1$ state of NO was measured. Because the population of the $v = 1$ state is likely to be the highest in the hot outer region of the boundary layer, the results of the test does not represent the vibrational temperature of the cold core flow. Therefore, this test result is omitted from discussion.

In Ref. 28, three different temperatures were measured in an arcjet wind tunnel: the rotational temperature, the maximum possible vibrational temperature of an excited state, and an electronic excitation temperature, all of NO. The measured temperatures are compared with the values calculated by the multitemperature model in Fig. 8. As seen in the figure, the measured rotational and vibrational temperatures are in close agreement with the calculations. But the measured electronic temperature is considerably higher than the calculated electronic temperature.

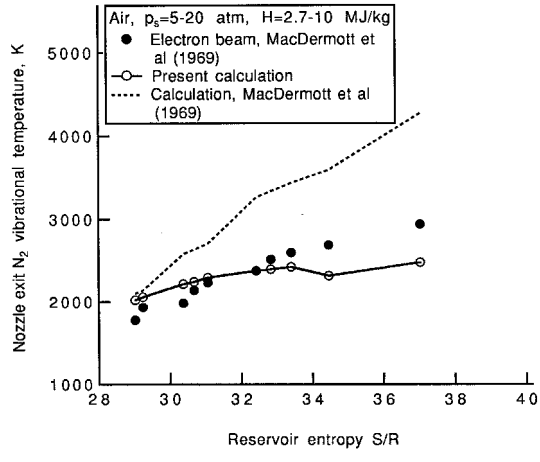

Fig. 7 Comparison between the measured[25] and calculated[26] vibrational temperatures of N_2 in air. The present calculation refers to the multitemperature calculation.[26]

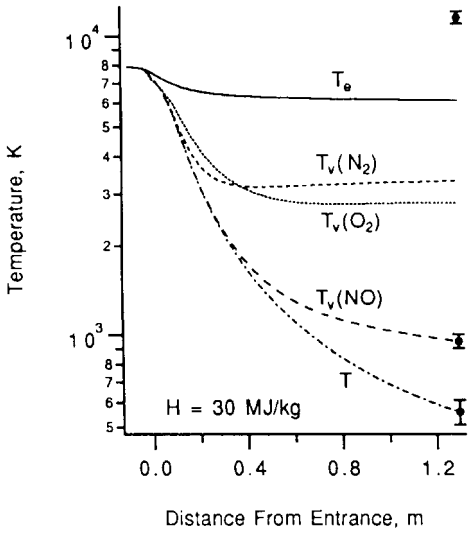

Fig. 8 Measured rotational temperature, vibrational temperature, and electronic excitation temperature of NO in an arcjet wind tunnel compared with a multitemperature calculation.[28]

Species Concentrations

It is possible to measure species concentrations in the test section of an arcjet wind tunnel using a mass spectrometer. Reference 2 cites two early works on this subject. Recently, a similar work was carried out by Schoenemann and Auweter-Kurtz.[29] However, none of the results of these investigations could be considered definitive. The only definitive results have been obtained so far by MacDermott and Dix.[30,31] In Fig. 9, their results are reproduced and compared with the calculations made with the conventional one-temperature model and the multitemperature model of Ref. 26. There is a fairly good agreement between the measurement and the multitemperature calculation. The one-temperature calculation produces a poor agreement.

In Fig. 10, the results for the 9.7-MJ/kg case in MacDermott's experiment[30,31] are compared with the multitemperature calculation along the nozzle. In the figure, the present calculation refers to the multitemperature calculation. The calculated value shows an increase in the mole fraction of atomic nitrogen along the nozzle and it agrees with the measured value at the nozzle exit. According to the hypothesis advanced in Ref. 26, this is a result of the enhancement of the rates of the two NO exchange reactions

$$O + N_2 \rightarrow NO + N(R1)$$

$$O + NO \rightarrow O_2 + N(R2)$$

by the excitation of vibrational and electronic modes. The rate coefficient of the reaction R1 is assumed in Ref. 26 to be a function only of electron–electronic temperature and that of R2 is assumed to be a function of an average temperature defined by $T_{av} = T_v^{0.1} T_e^{0.9}$.

The disagreement between the experimental data and the values calculated using the conventional one- or two-temperature model for arcjet flows was seen also for shock-tunnel flows. The species concentrations at the exit of a shock-tunnel nozzle were measured in Ref. 32 using a mass spectrometer. The measured values were very different from the values calculated using a one-temperature model. The measured O concentration was lower, the N concentration was much higher, and the NO concentration was higher than calculated. This trend is qualitatively the same as in the arcjet data shown earlier. However, the extent of disagreement is more severe for the shock-tunnel case. In Ref. 33, the measured data are fitted with a calculation based on the assumption that, in a shock

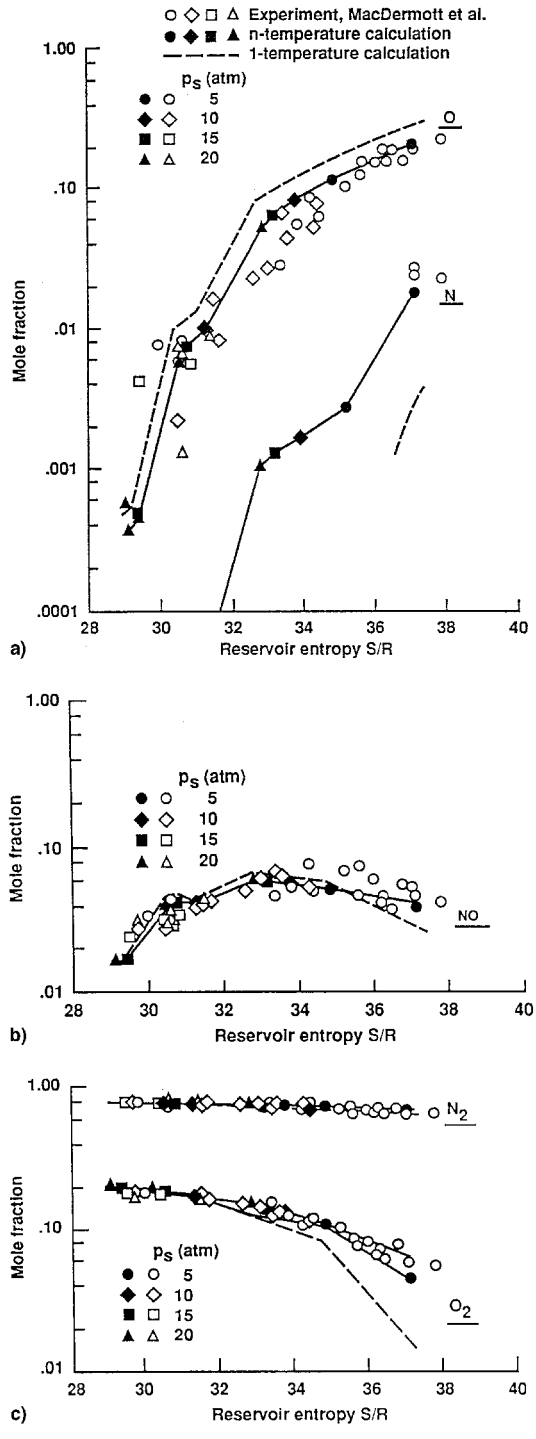

Fig. 9 Species mole fractions in an arcjet wind tunnel as a function of entropy. The *n*-temperature calculation refers to the multitemperature method in Ref. 26: a) O and N, b) NO, and c) O_2 and N_2.

tunnel 1) the three-body recombination rates are slower, and 2) the endothermic Zeldovich reactions occur with reduced activation energies. Assumption 2 made therein is qualitatively the same as that made in Ref. 26.

In Fig. 11, a summary comparison is made between the experimental data and the calculations mentioned earlier.[26] In the figure, the present calculation refers to the multitemperature calculation. The present rate coefficients refer to the rate coefficients given in Ref. 34. The NENZF rate coefficients refer to the rate coefficients given in Ref. 35. The figure shows that a multitemperature model is preferred over a one-temperature

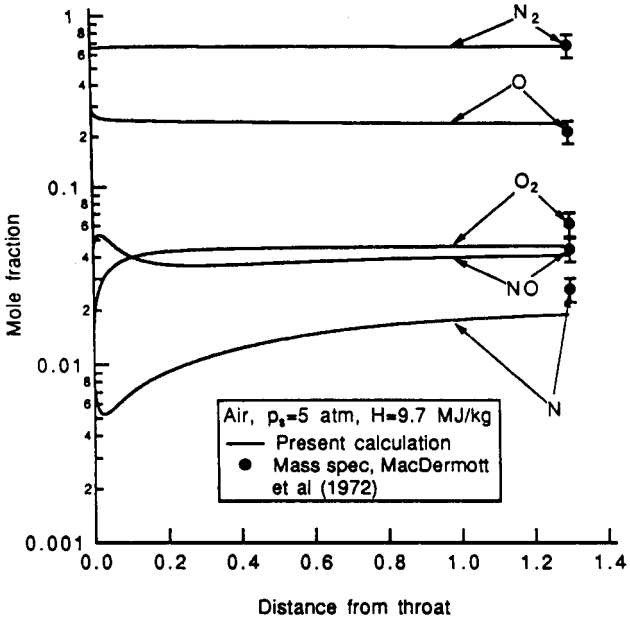

Fig. 10 Measured[31] and calculated[26] species concentrations along nozzle for p_s = 5 atm and H = 9.7 MJ/kg.

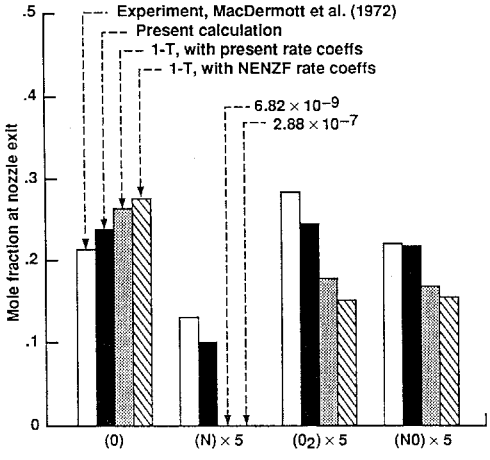

Fig. 11 Comparison between the measured[31] and calculated[26] species concentrations at nozzle exit at p_0 = 5 atm and H = 9.7 MJ/kg.

model in calculating the species concentrations in an arcjet wind tunnel.

Summary on Freestream Properties

The foregoing examination of the existing works leads one to the conclusion that the thermodynamic conditions in the freestream of an arcjet wind tunnel are substantially different from those calculated using the conventional one- or two-temperature model. Generally, vibrational and rotational temperatures agree with the calculations, provided the vibrational temperatures of O_2, N_2, and NO are separately calculated. However, the electronic temperature tends to be very high. The concentration of O atoms is significantly lower, that of NO molecules is significantly higher, and that of N atoms is very much higher than calculated. The flow velocity is also slower than calculated, which means that the energy content in the chemical mode is greater than calculated. Thus, the species and velocity measurements are consistent. A multitemperature model allowing for the effect of high electronic and vibrational temperatures is favored over the one- or two-temperature models in predicting the flow behavior.

This conclusion relies partly on the accuracy of the mass spectrometric measurements. A theoretical work on this subject[36] indicates that such measurements are affected by the surface-catalytic phenomena occurring on the walls of the lip of the instrument. For this reason, it is possible that the conclusions drawn here are erroneous. To confirm the accuracy of the present conclusion, it is desirable to carry out a nonintrusive measurement of species concentrations, such as that carried out in Ref. 37.

Conclusions

The contamination of the flow in an arcjet wind tunnel by copper vapor does not affect the measurements significantly. Enthalpy of the flow could best be determined by observing the radiation emanating from the shock layer over a flat disk and by analyzing the spectrum obtained. The product of the pitot total pressure and the disk diameter must be greater than 0.4 atm-cm for this method to be valid. The flows produced in the test section of an arcjet wind tunnel contains less atomic oxygen, more atomic nitrogen, and more nitric oxide molecules than calculated by the conventional model. A multitemperature model that accounts for the enhancement of the Zeldovich reactions as a result of electronically excited oxygen atoms can predict the species concentrations better.

References

[1]Horn, D. D., "Review of Existing Arc-Jet Wind Tunnels," Lecture Notes, AIAA Short Course on Aerothermodynamic Facilities and Measurement, Washington, DC, June 1994.

[2]Scott, C. D., "Survey of Measurements of Flow Properties in Arcjets," *Journal of Thermophysics and Heat Transfer*, Vol. 7, No. 1, 1993, pp. 9–24.

[3]Watson, V. R., and Pegot, E. B., "Numerical Calculations for the Characteristics of a Gas Flowing Axially Through a Constricted Arc," NASA TN D-4042, June 1962.

[4]MacDermott, W. N., Horn, D. D., and Fisher, C. J., "Flow Contamination and Flow Quality in Arc Heaters Used for Hypersonic Testing," AIAA Paper 92-4028, July 1992.

[5]Nicolet, W. E., Shepard, C. E., Clark, K. J., Balakrishnan, A., Kesselring, J. P., Suchsland, K. E., and Reese, J. J., Jr., "Analytical and Design Study for a High-Pressure, High-Enthalpy Constricted Arc Heater," Arnold Engineering Development Center, TR 75-47, Arnold Air Force Station, TN, 1975.

[6]Terrazas-Salinas, I., Park, C., Strawa, A. W., Gopaul, N. K. J. M., and Taunk, S., "Spectral Measurements in the Arc Column of an Arc-Jet Wind Tunnel," AIAA Paper 94-2595, June 1994.

[7]Durgapal, P., "Current Distribution in the Cathode Area of an Arcjet," *Journal of Thermophysics and Heat Transfer*, Vol. 7, No. 2, 1993, pp. 241–250.

[8]Durgapal, P., "Electrode Phenomena in High Current, High Pressure Arc Heaters," AIAA Paper 92-0810, Jan. 1992.

[9]Anderson, L. A., and Sheldahl, R. E., "Experiments with Two Flow Swallowing Enthalpy Probes in High-Energy Supersonic Streams," *AIAA Journal*, Vol. 9, No. 9, 1971, pp. 1804–1810.

[10]Winovich, W., "On the Equilibrium Sonic-Flow Method for Atmospheric Re-Entry Research," NASA TN D-2132, March 1964.

[11]Palumbo, G., Craig, R. A., and Carrasco, A., "Spectral Measurements of Shock Layer Radiation in an Arc-Jet Wind Tunnel," Instrument Society of America Meeting, Paper 93-145, Albuquerque, NM, Jan. 1993.

[12]Bamford, D. J., O'Keefe, A., Babikian, D. S., Stewart, D. A., and Strawa, A. W., "Characterization of Arc Jet Flows Using Laser-Induced Fluorescence," AIAA Paper 94-0690, Jan. 1994.

[13]Arepalli, S., Yuen, E. H., and Scott, C. D., "Application of Laser Induced Fluorescence for Flow Diagnostics in Arc Jets," AIAA Paper 90-1763, Jan. 1990.

[14]Marinelli, W. J., Kessler, W. J., Allen, M. G., Davis, S. J., Arepalli, S., and Scott, C. D., "Copper Atom Based Measurements of Velocity and Turbulence in Arc Jet Flows," AIAA Paper 91-0358, Jan. 1991.

[15]Fay, J. A., and Riddell, F. R., "Theory of Stagnation Point Heat Transfer in Dissociated Air," *Journal of Aerospace Sciences*, Vol. 25, No. 2, 1958, pp. 73–85.

[16]Goulard, R., "On Catalytic Recombination Rates in Hypersonic Stagnation Heat Transfer," *Jet Propulsion*, Vol. 28, No. 11, 1958, pp. 737–745.

[17]Park, C., "Assessment of Two-Temperature Kinetic Model for Ionizing Air," *Journal of Thermophysics and Heat Transfer*, Vol. 3, No. 3, 1989, pp. 233–244.

[18]Park, C., and Moore, D., "Polynomial Method for Determining Local Emission Intensity by Abel Inversion," NASA TN D-5677, Feb. 1970.

[19]Okuno, A. F., and Park, C., "Stagnation-Point Heat Transfer Rate in Nitrogen Plasma Flows: Theory and Experiment," *Journal of Heat Transfer*, Vol. 92, Series C, No. 3, 1970, pp. 372–384.

[20]Park, C., "Comparison of Electron and Electronic Temperatures in Recombining Nozzle Flow of Ionized Nitrogen-Hydrogen Mixture. Part 2. Experiment," *Journal of Plasma Physics*, Vol. 9, No. 4, 1973, pp. 217–234.

[21]Babikian, D. S., Craig, R. A., Palumbo, G., and Palmer, G., "Measured and Calculated Spectral Radiation from a Blunt Body Shock Layer in an Arc-Jet Wind Tunnel," AIAA Paper 94-0086, Jan. 1994.

[22]Babikian, D. S., Park, C., and Raiche, G. A., "Spectroscopic Determination of Enthalpy in Arc-Jet Wind Tunnel," AIAA Paper 95-0712, Jan. 1995.

[23]Blackwell, H. E., Yuen, E., Arepalli, S., and Scott, C. D., "Nonequilibrium Shock Layer Temperature Profiles from Arc Jet Radiation Measurements," AIAA Paper 89-1679, June 1989.

[24]Bamford, D., and Romanovsky, A., "Velocity and Chemical Composition Measurements in Arc Jet Flow," AIAA Paper 95-2039, June 1995.

[25]MacDermott, W. N., and Marshall, J. G., "Nonequilibrium Nozzle Expansion of Partially Dissociated Air: A Comparison of Theory and Electron-Beam Experiment," Arnold Engineering Development Center, TR-69-66, Arnold Air Force Station, TN, July 1969.

[26]Park, C., and Lee, S. H., "Validation of Multitemperature Nozzle Flow Code," *Journal of Thermophysics and Heat Transfer*, Vol. 9, No. 1, 1995, pp. 9–16.

[27]Howard, R. P., Dietz, K. L., McGregor, W. K., and Limbaugh, C. C., "Nonintrusive Nitric Oxide Density Measurements in the Effluent of Core-Heated Air Stream," AIAA Paper 90-1478, June 1990.

[28]Babikian, D. S., Gopaul, N. K. J. M., and Park, C., "Measurement and Analysis of Nitric Oxide Radiation in an Arcjet Fow," *Journal of Thermophysics and Heat Transfer*, Vol. 8, No. 4, 1994, pp. 737–743.

[29]Schoenemann, A., and Auweter-Kurtz, M., "Mass Spectrometric Investigation of High Enthalpy Plasma Flows," *Journal of Thermophysics and Heat Transfer*, Vol. 9, No. 4, 1995, pp. 620–628.

[30]MacDermott, W. N., and Dix, R. E., "Final Results of On-Line Spectrometric Analysis of Nonequilibrium Airflows," Arnold Engineering and Development Center, TR-71-23, Arnold Air Force Station, TN, Feb. 1971.

[31]MacDermott, W. N., and Dix, R. E., "Mass Spectrometric Analysis of Nonequilibrium Airflows," *AIAA Journal*, Vol. 10, No. 4, 1972, pp. 494–498.

[32]Skinner, K. A., "Mass Spectrometry in Shock Tunnel Experiments of Hypersonic Combustion," Ph.D. Dissertation, Univ. of Queensland, Australia, March 1994.

[33]Park, C., "Evaluation of Real-Gas Phenomena in High-Enthalpy Impulse Facilities: A Review," AIAA Paper 96-2207, June 1996.

[34]Park, C., "Assessment of Two-Temperature Kinetic Model for Ionizing Air," *Journal of Thermophysics and Heat Transfer*, Vol. 3, No. 3, 1989, pp. 233–244.

[35]Lordi, J. A., Mates, R. E., and Moselle, J. R., "Computer Program for the Numerical Solution of Nonequilibrium Expansions of Reacting Gas Mixtures," NASA CR-472, May 1979.

[36]Caram, J. M., Madden, C. B., Milhoan, J. D., Scott, C. D., Le Beau, G. J., Arepalli, S., Bouslog, S. A., and Urban, T. J., "Design of a Mass Spectrometer Probe Tip for the Arc-Jet Facility," AIAA Paper 94-0356, Jan. 1994.

[37]Meyer, S. A., Sharma, S. P., Bershader, D., Whiting, E. E., Exberger, R. J., and Gilmore, J. O., "Absorption Line Shape Measurement of Atomic Oxygen at 130 nm Using a Raman-Shifted Excimer Laser," AIAA Paper 95-0290, Jan. 1995.